

Journal Pre-proof

NMR-based metabolomics for frauds detection and quality control of oregano samples

Manuela Mandrone, Lorenzo Marincich, Ilaria Chiocchio, Alessandra Petrolì, Dejan Gođevac, Immacolata Maresca, Ferruccio Poli



PII: S0956-7135(21)00279-6

DOI: <https://doi.org/10.1016/j.foodcont.2021.108141>

Reference: JFCO 108141

To appear in: *Food Control*

Received Date: 15 January 2021

Revised Date: 10 March 2021

Accepted Date: 3 April 2021

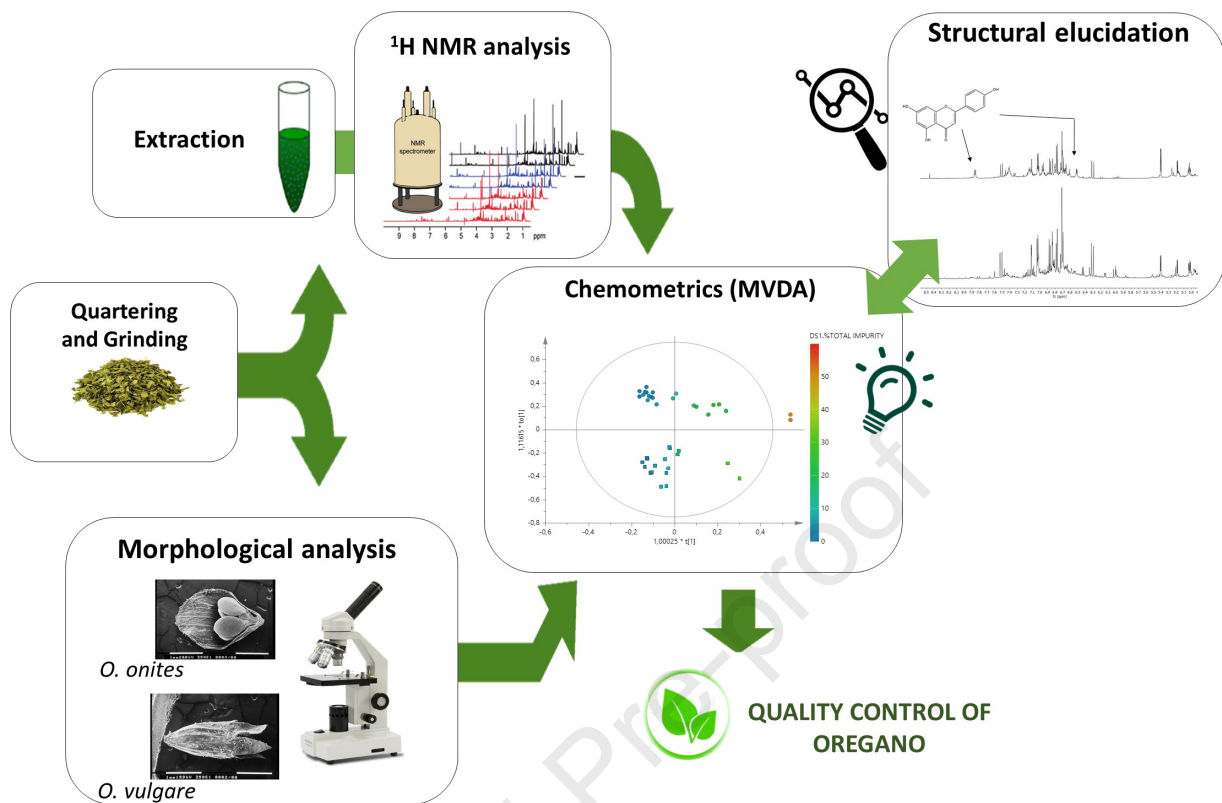
Please cite this article as: Mandrone M., Marincich L., Chiocchio I., Petrolì A., Gođevac D., Maresca I. & Poli F., NMR-based metabolomics for frauds detection and quality control of oregano samples, *Food Control*, <https://doi.org/10.1016/j.foodcont.2021.108141>.

This is a PDF file of an article that has undergone enhancements after acceptance, such as the addition of a cover page and metadata, and formatting for readability, but it is not yet the definitive version of record. This version will undergo additional copyediting, typesetting and review before it is published in its final form, but we are providing this version to give early visibility of the article. Please note that, during the production process, errors may be discovered which could affect the content, and all legal disclaimers that apply to the journal pertain.

© 2021 Published by Elsevier Ltd.

Author Contributions

Conceptualization: Manuela Mandrone (M.M.), Ferruccio Poli (F.P.); **Data curation:** M.M., Lorenzo Marincich (L.M.), Ilaria Chiocchio (I.C.); **Plant material authentication:** F.P.; Immacolata Maresca (I.M.); **Morphological Analysis and Microscopy:** I.M. and L.M.; **Metabolomics and Structure Elucidation:** M.M., I.C., L.M., Dejan Gođevac (D.G.); **Methodology:** M.M., L.M., Alessandra Petrolì (A.P.); **NMR Experimental design:** A.P., M.M.; **Investigation:** M.M., I.C., L.M., F.P., D.G.; **Software:** M.M., A.P., L.M.; **Funding acquisition:** F.P.; **Project administration:** M.M. and F.P.; **Supervision:** M.M. and F.P.; **Writing – original draft:** M.M., L.M., I.C.; **Writing – review & editing:** M.M., F.P., D.G. All authors have read and agreed to the published version of the manuscript.



1 **NMR-based metabolomics for frauds detection and quality control of oregano samples**

2 Manuela Mandrone^{a*}, Lorenzo Marincich^a, Ilaria Chiocchio,^a Alessandra Petroli^b, Dejan Gođevac^c,
3 Immacolata Maresca^d, Ferruccio Poli^a

4
5 ^aDepartment of Pharmacy and Biotechnology, University of Bologna, Via Irnerio, 42, 40126 Bologna, Italy

6 ^bDepartment of Industrial Chemistry, University of Bologna, Viale del Risorgimento, 4, 40136 Bologna, Italy

7 ^cDepartment of Chemistry, Institute of Chemistry, Technology, and Metallurgy, University of Belgrade,
8 Njegoševa 12, 11000 Belgrade, Republic of Serbia

9 ^dDepartment of Life Sciences and Biotechnology, University of Ferrara, via Borsari 46, 44100 Ferrara, Italy

10

11

12

13 ***Correspondence**

14 Dr. Manuela Mandrone, University of Bologna, Department of Pharmacy and Biotechnology, Via
15 Irnerio 42, 40126 Bologna, Italy

16 E-mail: manuela.mandrone2@unibo.it Phone: +390512091294; Fax +39051242576

17

18

19

20

21 Abstract

22 In this work ¹H NMR metabolomics has been employed for quality control of oregano samples. NMR
23 data and morphological analysis (MA) were combined by PCA, obtaining a model able to individuate
24 non-marketable samples, and to distinguish between the two marketable oregano species (*Origanum*
25 *vulgare* and *O. onites*) on the basis of their metabolomic profile. Through this approach distinctive
26 biomarkers of the two species were found, namely apigenin and p-cymene for *O. onites*, and salvianolic
27 acid B for *O. vulgare*. Furthermore, the percentage of the samples' impurity (evaluated by MA) and the
28 metabolomic profiles were correlated by OPLS models, which showed that, in addition to the species-
29 specific biomarkers, thymol and rosmarinic acid (common to both marketable species) strongly
30 correlate to oregano degree of purity. Cistus was one of the most frequent contaminants, thus, a further
31 OPLS model, able to detect the degree of cistus contamination in oregano samples, was also built.

32

33 Keywords

34 NMR-based metabolomics; quality control; biomarkers; apigenin; p-cymene; salvianolic acid B;
35 oregano; cistus

36

37 Chemical compounds studied in this article:

38 Apigenin (PubChem CID: 5280443); Carvacrol (PubChem CID: 10364); p-Cymene (PubChem CID:
39 7463); Rosmarinic acid (PubChem CID: 5315615); Salvianolic acid B (PubChem CID: 11629084);
40 Thymol (PubChem CID: 6989)

41

42 **List of abbreviations**

43 **MA:** morphological analysis

44 **MVDA:** multivariate data analysis

45 **NMR:** nuclear magnetic resonance

46 **OPLS:** orthogonal partial least squares

47 **OPLS-DA:** orthogonal partial least squares discriminant analysis

48 **PCA:** principal components analysis

49 **VIP:** variable influence on projection

50

51 **1. Introduction**

52 The global herbs and spices market is increasingly threatened by accidental or intentional adulteration,
53 also facilitated by the complexity of the supply chains (Galvin-King et al., 2018). Herbs are generally
54 sold chopped or powdered, making it relatively easy to counterfeit by means of adding cheaper bulking
55 agents (i.e. chemicals, extraneous material from other plants or foreign species) (Van Ruth et al., 2018).
56 In this scenario, the development of rapid, robust, cost-effective and environmentally friendly methods
57 for authentication and quality control of spices and herbs takes on great importance (Wadood et al.
58 2020).

59 Oregano is one of the most adulterated herbs (Black *et al.*, 2016; L. Drabova et al., 2019). Despite the
60 high heterogeneity of *Origanum* genus, only a few species are accepted on the market. According to
61 ISO 7925:1999, all *Origanum* species and sub-species, except *Origanum majorana* L. are considered
62 marketable, while according to the European Spice Association (ESA) only *Origanum vulgare* L. and

63 *Origanum onites* L. (or products made of a mixture of the two) are considered ‘true’ oregano (List of
64 culinary herbs and spices, ESA, 2018), with the limit of permitted impurities set at 2% (w/w) (Quality
65 minima document, ESA, 2015). With respect to oregano authentication, the European Pharmacopoeia
66 makes a further restriction: in addition to *O. onites*, it only considers a specific subspecies (subsp.) of
67 *O. vulgare* as ‘true’ oregano, namely *O. vulgare* subsp. *hirtum* (Link) Ietsw (9th European
68 Pharmacopoeia, 2017).

69 Besides the frauds ascribable to the sale of non-marketable species, oregano is often contaminated with
70 a significant amount of other plants such as olive tree leaves, myrtle, sumac, cistus, savory and others
71 (Black et al. 2016, Marieschi et al., 2009; Marieschi et al., 2010; Marieschi et al., 2011a; Marieschi et
72 al., 2011b).

73 Generally, companies dealing with large-scale sales buy oregano from third parties. The contractor
74 sends a representative sample and the company analyzes it in order to establish, on the basis of the
75 sample quality, whether to buy it or not. In this stage, in order to determine the authenticity and purity
76 of samples, companies generally rely on morphological analysis performed by microscopy (MA).
77 Nevertheless, this technique is time-consuming, and thus not suitable for quickly analyzing a high
78 number of samples; furthermore, its precision strongly depends on the operator performing the
79 analysis. This makes it of great importance to develop new efficient, quick and cost-affordable methods
80 for oregano quality control, and to contribute to building databases, apt to facilitate fraud detection
81 worldwide.

82 Marieschi et al. (2009, 2010, 2011a, 2011b) published several works focused on the assessment of
83 oregano authenticity by sequence-characterized amplified region markers (SCARs), which also allowed
84 them to recognize a number of specific adulterants. The technique proposed is extremely precise and
85 accurate, however, it does not provide information about the phytochemical features of the samples,

86 which is a further element of interest to establish the quality of an herbal product. In fact, the presence
87 of specific metabolites confers the characteristic taste and flavor to the herb. Moreover, several plant
88 secondary metabolites are organ-specific, this implies, taking for instance the case of oregano, that a
89 high-quality sample should be made of leaves and bracts predominantly, with the lowest possible
90 amount of stem. Hence, the analysis of the phytochemical profile is an important additional step for the
91 quality assessment of herbs, also considering that the metabolites production in plants is significantly
92 affected by a number of factors, including seasonal variation, altitude, biotic and abiotic factors and so
93 on (Mandrone et al 2021, Anđelković et al., 2017; Scognamiglio et al., 2015; Salomè et al., 2020).

94 In the field of phytochemistry applied to food or herb quality control, in addition to targeted analysis,
95 new untargeted strategies, relying on an inductive approach, have recently been emerging. In this case,
96 the analytical protocols used are set to detect the widest possible range of metabolites (metabolome)
97 (Riedl et al., 2015). According to this approach, the insights are gained from comparison, on a pattern
98 level, of a high number of samples by multivariate data analysis (MVDA). This workflow was
99 successfully applied by Black et al. (2016) to determine oregano quality by both FTIR and LC-HRMS
100 untargeted analysis. In this context, a further analytical option is offered by NMR-based metabolomics,
101 increasingly employed for untargeted food and herbs quality control (Sobolev et al., 2019). NMR is
102 non-destructive, quickly performed and environmental-friendly, and in addition it provides numerous
103 detailed chemical information in a single spectrum (Pontes et al., 2017).

104 This study explores the potentiality of ^1H NMR metabolomics to be employed for oregano quality
105 control. In particular, spectral data and results obtained by MA (performed by stereomicroscope and
106 optical microscope) were combined by MVDA. Predictive multivariate data models, able to quickly
107 provide a wide spectrum of information on oregano samples, were obtained, and oregano biomarkers of
108 quality easily detectable by ^1H NMR profiling were identified.

109

110 **2. Methods and material**

111 **2.1 Chemicals**

112 Deuterium oxide (D₂O, 99.90% D), CD₃OD (99.80% D) were purchased from Eurisotop (Cambridge
113 Isotope Laboratories, Inc, France). Standard 3-(trimethylsilyl)-propionic-2,2,3,3-*d*₄ acid sodium salt
114 (TMSP), sodium phosphate dibasic anhydrous and sodium phosphate monobasic anhydrous and all the
115 other chemicals and solvents were purchased from Sigma-Aldrich Co. (St. Louis, MO, USA).

116 **2.2 Oregano samples and *Cistus creticus***

117 Different Italian companies provided a total of twenty-seven samples of (supposed) oregano to be
118 analyzed in order to assess purity and authenticity. According to what declared by the companies: 14
119 samples were cultivated in Turkey, 3 in Sicily, 3 in Albania, 2 in Peru, while for 5 samples this
120 information was not available. Vouchers of crude drugs were deposited in Department of Pharmacy
121 and Biotechnology, University of Bologna (via Imerio 42, Bologna, Italy) and reported in Table 1,
122 together with the results obtained by the MA performed in this work.

123 *Cistus creticus* (ex. *incanus*) L. was harvested on April 2017 in Ostuni (Brindisi, Italy; 40°43'31.153"
124 N 17°35'27.844" E), the sample was identified by F.P., and voucher specimen (BOLO0602029) was
125 retained at the Herbarium of Alma Mater Studiorum University of Bologna (SMA) (Via Imerio 42,
126 40126, Bologna, Italy).

127 **2.3 Morphological analysis**

128 The identification of oregano species was performed according to the oregano taxonomic key presents
129 in Ietswaart (1980). Morphological analysis (MA) was performed following the method reported by
130 Marieschi et al. 2009. In particular, twenty-five milligrams of each dried sample were analyzed by a

131 stereoscopic microscope (Nikon SMZ-1000) and a microscope (Nikon Eclipse E600). The pictures
132 were obtained by Scanning Electron Microscopy. Specifically, dried calices of *Origanum onites* and
133 *Origanum vulgare* were mounted on aluminum stubs with double-stick carbon tape, sputter coated with
134 gold nanoparticles (5 nm) using a Emitech K500 coater and observed with a Philips SEM 515 at 20.0
135 and 19.9 kV respectively.

136 **2.4 Sample preparation for metabolomics**

137 Samples were constituted by dried and shredded plant material. They were quartered and powdered
138 using an electrical grinder (IKA, A11 basic, Merck, Italy) Then 50 mg were extracted with 1 mL of
139 mixture (1:1) of phosphate buffer (90 mM; pH 6.0) in H₂O-*d*₂ (containing 0.1% TMSP) and MeOH-*d*₄
140 by ultrasonication (TransSonic TP 690, Elma, Germany) for 20 minutes at 45°C. After this procedure,
141 samples were centrifuged for 10 min (17000 x *g*), then 700 µL of supernatant were transferred into
142 NMR tubes. For each sample, two different extracts were prepared to test reproducibility.

143 **2.5 NMR and ESI-MS measurement**

144 ¹H NMR spectra, *J*-resolved (*J*-res), ¹H-¹H homonuclear (COSY) and inverse detected ¹H-¹³C
145 correlation experiments (HMBC, HSQC) were recorded at 25°C on a Varian Inova instrument
146 (equipped with a reverse triple resonance probe). For ¹H NMR profiling the instrument was operating
147 at ¹H NMR frequency of 600.13 MHz, and H₂O-*d*₂ was used as internal lock. Each ¹H-NMR spectrum
148 consisted of 256 scans (corresponding to 16 min) with the relaxation delay (RD) of 2 s, acquisition time
149 0.707 s, and spectral width of 9595.8 Hz (corresponding to δ 16.0). A presaturation sequence
150 (PRESAT) was used to suppress the residual water signal at δ 4.83 (power = -6dB, presaturation delay
151 2 s). For 1D and 2D NMR analysis of pure compounds MeOH-*d*₄ was used as lock. *J*-res spectra has
152 been measured in order to clarify or confirm splitting patterns and coupling constants values. This

153 approach is especially useful in metabolomics where a mixture of compounds is visible in a single ^1H
154 NMR spectrum making more difficult to establish these parameters (Emwas et al, 2019).

155 For ESI-MS analyses, dried pure compounds were dissolved in MeOH, and analyzed by WATERS ZQ
156 4000 (Milford, MA USA) mass spectrometer. in negative and/or positive ion modes according to the
157 more ionizable chemical groups of samples. A direct infusion of 20 $\mu\text{L}/\text{min}$, source temperature of 80
158 $^{\circ}\text{C}$ and desolvation (nitrogen) gas (flow rate of 200 L/h) were common parameters used in both
159 positive and negative ion modes. Capillary potential and source cone were 3.54 Kv and 20 V in
160 positive ion mode, and 2.53 Kv and 30 V in negative ion mode. The mass range was from 0 to 1000
161 m/z .

162 **2.6 Multivariate data analysis**

163 The spectra were manually phased and baseline corrected, and calibrated to the internal standard
164 trimethyl silyl propionic acid sodium salt (TMSP) at δ 0.0 using Mestrenova software (Mestrelab
165 Research, Spain). The regions of δ 5–4.5 and δ 3.34–3.30 were excluded from the analysis because of
166 the residual solvent signals. Then spectral intensities were reduced to integrated regions of equal width
167 (δ 0.04) corresponding to the region from δ 0.0 to 10.0, and normalized by total area.

168 The analysis of ^1H NMR profiles of extracts was performed based on an in-house library and
169 comparison with literature (Mandrone et al., 2017; Mandrone et al., 2019b).

170 SIMCA P+ software (v. 15.0, Umetrics, Sweden) was used in order to perform PCA, OPLS, OPLS-
171 DA, PLS-DA models. For multivariate analysis, data were subjected to Pareto scaling. Supervised
172 models were evaluated by the goodness of fit (R^2x (cum) and R^2y (cum)) and goodness of prediction
173 (Q^2 (cum)), together with the parameters given by cross validation tests: permutation test (performed
174 using 200 permutations) and CV-ANOVA (Malzert-Fréon et al., 2010).

175 2.7 Purification and structure elucidation of biomarkers

176 In order to elucidate the structure of the metabolites of interest, different NMR-guided isolation
177 procedures were carried out for *O. onites*, *O. vulgare* and *Cistus creticus*. The NMR spectra of the
178 isolated compounds and/or fractions are given in supporting material (Fig. S1 to S8).

179 2.6.1 Isolation of biomarkers from *O. onites* and *O. vulgare*

180 Forty g of *O. onites* (degree of purity of 99.88%) or *O. vulgare* (degree of purity of 98.74%) were
181 extracted using 300 mL of CH₃OH:H₂O (1:1), sonicating for 30 min and centrifuging for 10 min
182 (2469 x g). The obtained supernatant was dried in rotary evaporator at 40°C yielding 18% w/w for
183 *O. onites* and 15% for *O. vulgare*. In both cases, the dry extract was suspended into 300 mL of water
184 to undergo liquid-liquid partition with CHCl₃, EtOAc and *n*-BuOH used in sequence, repeating the
185 procedure twice for each solvent. Fractions were dried in rotary evaporator, and for *O. onites* 5 g
186 were obtained from the water fraction, 1.5 g from the *n*-BuOH fraction, 0.36 g from the EtOAc
187 fraction, and 0.2 g from the CHCl₃ fraction. While for *O. vulgare* 4.50 g were obtained from the
188 water fraction, 0.96 g from the *n*-BuOH fraction, 0.27 g from the EtOAc fraction and 0.22 from the
189 CHCl₃ fraction.

190 The biomarkers of *O. onites* were found (by ¹H-NMR analysis) in the CHCl₃ and the *n*-BuOH
191 fractions, while the water fraction contained the biomarker of *O. vulgare*. Fractions in EtOAc
192 obtained from both species contained rosmarinic acid, whose structure was elucidated by NMR and
193 ESI-MS experiments (Exarchou, et al. 2003). The CHCl₃ fraction obtained from *O. onites* was
194 analyzed by ¹H NMR and ESI-MS (by direct infusion) allowing to confirm the structures of thymol
195 and p-cymene (Exarchou, et al. 2003). For purification and structure elucidation, 200 mg of *n*-BuOH
196 and water fractions from *O. onites* and *O. vulgare*, respectively, were further fractionated by column
197 chromatography, using in both cases a chromatography column (1800 mm x 25 mm) filled with 220

198 g of Sephadex (LH-20) and, as eluent, methanol. The fractions were suspended in the minimum
199 amount of CH₃OH:H₂O (1:1) to be chromatographed. The flow rate was of 0.4 mL/min. Each
200 fraction was concentrated and analyzed by ¹H-NMR. Fraction 114 contained the biomarker of
201 interest of *O. onites*, which has been identified as apigenin (0.1 mg) (Exarchou, et al. 2003). In case
202 of *O. vulgare* fractions from 25 to 27 contained the biomarker of interest identified as salvianolic
203 acid B (10.9 mg) (Sun et al., 2009). Table S1 summarizes the results of the NMR experiments
204 performed in order to elucidate the structure of salvianolic acid B (¹H NMR, HMBC, HSQC,
205 COSY).

206 2.7.2 Isolation of pinitol as biomarker of *C. creticus*

207 In order to characterize the biomarker of *Cistus creticus* L., 9.8 g of dried and grounded plant
208 material were extracted using 300 mL of CH₃OH:H₂O (1:1); sonicated for 40 min; centrifuged for
209 10 min (2469 x g). This extraction procedure was repeated twice on the same plant material. The
210 extract was dried in rotary evaporator (yield = 30.6% w/w) and suspended in 300 mL of water to
211 undergo liquid-liquid partition with CHCl₃ and EtOAc (for two times each), obtaining 2.9 g of
212 material from the water fraction and 0.1 g from the EtOAc fraction. According to ¹H-NMR analysis,
213 water fraction contained the metabolite of interest, thus 300 mg of this fraction were suspended in
214 500 µL of water and injected in MPLC instrument (Reveleris®, Büchi, Switzerland) connected to
215 C₁₈ column (4 g). A gradient of water (solvent A) and methanol (solvent B) was used as eluent. The
216 steps gradient was composed by an isocratic phase of 10 min (95% A and 5% B), a gradient from
217 95% A to 90% A in 10 min, an isocratic phase of 10 min (90% A and 10% B), a gradient from 90%
218 A to 80% A in 10 min, an isocratic phase of 10 min (80% A and 20% B), a gradient from 80% A to
219 0% A in 20 min. The flow rate was 3 mL/min, and the run length was 70 minutes. A total of 43

220 fractions were collected, and the metabolite of interest was found in was in fraction 3 and fraction 4.

221 NMR and MS analysis suggested that this compound might be pinitol.

222 Apigenin ^1H NMR (D_2O , 600 MHz): δ 7.80 (d, 2, $J = 9.06$ Hz, H-2', H-6'), 6.88 (d, 2, $J = 9.06$ Hz, H-
223 3', H-5'), 6.47 (s, 1, H-3), 6.27 (d, 1, $J = 2.25$ Hz, H-8), 6.07 (d, 1, $J = 2.25$ Hz, H-6). Negative ESI-
224 MS m/z : 269 $[\text{M} - \text{H}]^-$ calculated as 270.24 for $\text{C}_{15}\text{H}_{10}\text{O}_5$.

225 p-Cymene ^1H NMR (CD_3OD , 600 MHz): δ 7.34 (d, 2, $J = 8.95$ Hz), 7.12 (d, 2, $J = 8.95$ Hz), 2.79 (m,
226 1), 1.98 (s, 3), 0.99 (d, 6, $J = 6.79$ Hz). Negative ESI-MS m/z : 133 $[\text{M} - \text{H}]^-$ calculated as 134.21 for
227 $\text{C}_{36}\text{H}_{30}\text{O}_{16}$.

228 Rosmarinic acid ^1H NMR (CD_3OD , 600 MHz): δ 7.52 (d, 1, $J = 15.90$ Hz), 7.01 (d, 1, $J = 1.91$ Hz),
229 6.93 (dd, 1, $J = 1.91, 8.21$ Hz), 6.75 (d, 1, $J = 8.21$ Hz), 6.72 (d, 1, $J = 1.91$ Hz), 6.67 (d, 1, $J = 8.21$
230 Hz), 6.59 (dd, 1, $J = 1.91, 8.21$ Hz), 6.24 (d, 1, $J = 15.90$ Hz), 5.16 (dd, 1, $J = 4.28, 8.51$ Hz), 3.07 (dd,
231 1, $J = 4.28, 14.39$ Hz), 2.98 (dd, 1, $J = 8.51, 14.39$ Hz). Negative ESI-MS was performed on EtOAc
232 fraction of *O. vulgare*, yielding m/z : 359 $[\text{M} - \text{H}]^-$ calculated as 360.31 for $\text{C}_{18}\text{H}_{16}\text{O}_8$.

233 Salvianolic acid B ^1H NMR (CD_3OD , 600 MHz): δ 6.94 (d, 1, $J = 8.54$ Hz), 6.91 (d, 1, $J = 16.27$ Hz),
234 6.86 (d, 1, $J = 8.54$ Hz), 6.85 (d, 1, $J = 2.33$ Hz), 6.84 (d, 1, $J = 2.33$ Hz), 6.82 (d, 1, $J = 8.54$ Hz), 6.81
235 (d, 1, $J = 8.54$ Hz), 6.74 (dd, 1, $J = 8.54, 2.33$ Hz), 6.70 (dd, 1, $J = 8.54, 2.33$ Hz), 6.35 (d, 1, $J = 8.54$
236 Hz), 6.17 (d, 1, $J = 2.33$ Hz), 6.00 (d, 1, $J = 8.54, 2.33$ Hz), 5.90 (d, 1, $J = 5.82$ Hz), 5.79 (d, 1, $J =$
237 16.27 Hz), 4.93 (dd, 1, $J = 10.10, 3.54$ Hz), 4.83 (dd, 1, $J = 12.11, 3.94$ Hz), 4.33 (d, 1, $J = 5.82$ Hz),
238 3.04 (dd, 2, $J = 14.44, 3.54$ Hz), 2.92 (dd, 2, $J = 14.70, 12.11$ Hz), 2.85 (dd, 2, $J = 14.44, 10.10$ Hz),
239 2.49 (dd, 2, $J = 14.70, 3.94$ Hz). Negative ESI-MS m/z : 717 $[\text{M} - \text{H}]^-$ calculated as 718.6 for
240 $\text{C}_{36}\text{H}_{30}\text{O}_{16}$.

241 Thymol ^1H NMR (CD_3OD , 600 MHz): δ 6.9 (d, 1, $J = 7.55$ Hz), 6.59 (d, 1, $J = 1.23$ Hz), 6.56 (dd, 1, J
242 = 1.23, 7.55 Hz), 2.73 (m, 1), 2.10 (s, 3), 1.16 (d, 6, $J = 6.95$ Hz). Negative ESI-MS was performed on
243 CHCl_3 fraction of *O. onites*, yielding m/z : 149 $[\text{M} - \text{H}]^-$ calculated as 150.22 for $\text{C}_{10}\text{H}_{14}\text{O}$.

244 3. Results and Discussion

245 3.1 Discrimination between *Origanum* species

246 The samples analyzed in this work were provided by different companies, who, in turn, obtained them
247 from third parties. The samples were under evaluation by the companies in order to decide whether to
248 buy and put them on the market or not. These samples were subjected both to MA and ^1H NMR
249 profiling. Species, percentage of stem, degree of total impurity, and percentage of specific
250 contaminants were firstly assessed by MA, as usually done by the companies in order to verify the
251 quality and the authenticity of the samples (Table 1).

252 The most evident morphological difference between *O. vulgare* and *O. onites* is the shape of their
253 calices, *O. vulgare* is characterized by actinomorphic calix (radial symmetry), with five equal lobes
254 (teeth), while *O. onites* presents a cone shaped zygomorphic calyx (with only one plane of symmetry,
255 bilaterally symmetrical) open on one side (Fig. 1A) (Ietswaart, 1980). According to the MA analysis,
256 out of twenty-seven samples, twelve were *O. vulgare*, eleven *O. onites*, two samples resulted composed
257 by a mixture of the two species, and two were recognized as non-marketable species.

258 After recording the ^1H NMR spectra, a first overview of the results obtained was acquired by
259 performing Principal Components Analysis (PCA), using bucketed ^1H NMR spectra as x variables. The
260 results obtained by PCA analysis agreed with what observed by MA, except for the samples coming
261 from Sicily, thus they were excluded from the first PCA model developed (this result will be discussed
262 later in the text). Excluding all unknown species, sixteen components (PCs) maximized the explained

263 98.6% of the variance in the data set (given by $R^2x(\text{cum})$), while the obtained $Q^2(\text{cum})$ was 89.6%,
264 indicating very good predictability (Q^2 must be equal or higher than 50%). This PCA model facilitated
265 the detection of similarities/differences among the metabolomic profiles of the samples. As highlighted
266 by the score scatter plot (Fig. 1A), the model was able to make a distinction between the two
267 marketable oregano species along the component t[1], and, consistently, the samples made up of the
268 two species blended were placed in the middle of the plot (violet dots). On the other hand, the shift
269 along the component t[2] was due to sample degree of purity, which decreases along positive t[2].

270 In order to facilitate the identification of the main biomarkers responsible for the differentiation
271 between the two marketable species, an OPLS-DA (Orthogonal Partial Least Squares-Discriminant
272 Analysis) model was build (Fig. 1B), using as discriminant classes the two species of oregano (*O.*
273 *onites* and *O. vulgaris*) previously identified by MA. Considering the objective of this analysis, the
274 model was performed excluding from the data set the samples constituted by the mix of the two
275 species, and the samples heavily adulterated with other herbs (percentage of contamination higher than
276 15%).

277 The OPLS-DA analysis find a perfect fit to the response using two components, with goodness of fit
278 ($R^2y(\text{cum})$) of 100% and goodness of prediction ($Q^2(\text{cum})$) of 98.5%. Considering that these two
279 parameters have to be as close as possible to 100% (Malzert-Fréon et al., 2010), the obtained model is
280 interpretable and strongly predictable. This was further confirmed by permutation test (200
281 permutations) (Fig. S9), giving $Q^2(\text{cum})$ of 99% and intercept on y axis of Q -line of -0.55; while
282 $R^2(\text{cum})$ was 99% and intercept on y axis of R -line was 0.19, and significance testing of the model
283 based on ANOVA of the cross-validated residuals (CV-ANOVA) giving $p = 4.64 \times 10^{-17}$ and $F = 313$.

284 Loading plot and S -plot of OPLS-DA model show the relationships between x variables and sample
285 classes, in this case, x were ^1H NMR spectral signals and classes were oregano species (Fig. S9). In

286 order to elucidate the molecular structure of the metabolites responsible for these ^1H NMR signals, they
287 were isolated by NMR-guided fractionation and subjected to 1D, 2D-NMR and ESI-MS analysis. After
288 this procedure, salvianolic acid B was found to be a biomarker of *O. vulgare*, while the flavonoid
289 apigenin and the terpene p-cymene resulted the biomarkers of *O. onites* (Fig. 2 and Fig. S10). To the
290 best of our knowledge, this is the first detailed report of the main biomarkers useful to distinguish
291 between these two oregano species. Although also Blake et al. 2016 developed a method to detect
292 adulteration in oregano samples through both FTIR and LC-HRMS untargeted analysis, their results are
293 only at a pattern level, while no biomarkers identification was reported in their work.

294 The significance of the identified biomarkers was confirmed by their variable influence on projection
295 (VIP) scores: p-cymene (VIP=1.60; calculated for signal at δ 0.98); apigenin (VIP=1.58; δ 6.51);
296 salvianolic acid B (VIP=1.67; δ 6.35).

297 Other aromatic signals (number 15 in Fig. 2) emerged from the OPLS-DA as characteristic of *O.*
298 *onites*, however, the metabolite(s) responsible for these signals was not fully characterized in this work.

299 Besides the possibility to discriminate between *O. vulgare* from *O. onites*, metabolomics also
300 individuated non-marketable samples. This was highlighted when the two samples, classified by MA as
301 unknown plant material (thus non-marketable), were added to the data matrix and processed by PCA.
302 These samples resulted, in fact, outliers (Fig. 1C), since their phytochemical profile was completely
303 different from the marketable oregano species. In this specific case, the non-marketable samples were
304 lacking the main components of the essential oil (among which thymol), and they showed a different
305 aromatic pattern, with high content of amino acid tyrosine, which was not detected in marketable
306 oregano species (Fig. S11). Conversely, rosmarinic acid was detected both in 'true oregano' and in
307 these non-marketable samples.

308 As above described, the results obtained by PCA and successively by OPLS-DA were consistent with
309 those obtained by MA, making reliable the discrimination of oregano species based on their ^1H NMR
310 profiles. However, in this study, the results of MA and NMR-metabolomics disagreed on three samples
311 (all three coming from Sicily), which were classified by MA as *O. vulgare* (based on morphological
312 traits), these samples resulted extremely different from both *O. vulgare* and *O. onites* when analyzed by
313 NMR-based PCA (Fig. 3A). Thus, according to metabolomics approach, these samples should be
314 considered non-marketable. In particular, instead of thymol (which was not detected) they were
315 enriched in carvacrol, which was not found in the NMR profiles of marketable oregano species (Fig.
316 3B-C). These two positional isomers were easily distinguished by ^1H NMR spectroscopy, in fact, the
317 signal of the methyl group (in *para* position to the isopropyl group on the aromatic ring) of carvacrol is
318 more downfield shifted (δ 2.22) compared to the spectrum of its positional isomer thymol (δ 2.14) (Fig.
319 3C). This spectral feature is due to the β -effect of the hydroxyl group. Conversely, the spectral signal of
320 the same substituent in thymol resulted de-shielded, since the hydroxyl group decreases electron
321 density due to smaller inductive and resonance effect.

322 These samples are likely a Sicilian subspecies of *O. vulgare* (or a chemotype), hardly recognizable by
323 dichotomous keys. This result highlights the potentialities of NMR-based metabolomics approach for
324 oregano quality control.

325 3.2 Assessment of samples degree of purity

326 Two independent OPLS models were built (one for each species of marketable oregano), using as y
327 variable the percentage of total impurity found in the samples by MA (Fig. 4A-B).

328 For *O. vulgare*, the model was fitted by six components ($R^2x(\text{cum}) = 90.4\%$, $R^2y(\text{cum}) = 96.9\%$, and
329 $Q^2(\text{cum}) = 91.1\%$). Its predictability was confirmed by $R^2(\text{cum})$ and $Q^2(\text{cum})$ obtained by permutation
330 test (200 permutations), which were 96.9% and 91.1%, respectively, while intercept on y axis of Q -line

331 was -1.38, of R -line intercept was 0.696. CV-ANOVA F and p were 9.11 and 0.002, respectively. The
332 value of R^2 obtained in the observed vs predicted plot was 0.9695, indicating a consistency between
333 prediction based on NMR profiling and observations made by MA (Fig. 4A). However, one sample
334 (BO19UOR in Table 1) was considered less pure than what was established by MA, this result might
335 be explained by the content of stem (found in this sample), which likely lower the amount of the
336 biomarkers, leading the model to classify it as less pure.

337 For *O. onites*, the model was fitted by four components ($R^2x(\text{cum}) = 79.2\%$, $R^2y(\text{cum}) = 98.8\%$, and
338 $Q^2(\text{cum}) = 96.1\%$). Its predictability was confirmed by $R^2(\text{cum})$ and $Q^2(\text{cum})$ obtained by permutation
339 test (200 permutations), which were 98.8% and 96%, respectively, while intercept on y axis of Q -line
340 was -1.07, of R -line intercept was 0.478, and $F = 39.85$ and $p = 6.5 \times 10^{-8}$ by CV-ANOVA. The value
341 of R^2 obtained for observed vs predicted plot was 0.9883, indicating, also in this case, a consistency
342 between NMR profiling and MA results, with some discrepancies especially at very low level of
343 impurity (Fig. 4B, S12).

344 The OPLS models, built for the two *Origanum* species, individuated thymol and rosmarinic acid as
345 important biomarkers of purity. Thymol had a VIP coefficient (calculated for the signal at δ 2.14) of
346 2.19 for *O. onites* and 2.41 for *O. vulgare*. Rosmarinic acid VIP coefficient (δ 7.11) was 1.69 and 1.60
347 for *O. onites* and *O. vulgare*, respectively. These two compounds were easily recognizable by ^1H NMR
348 profiling, however their molecular structures were confirmed by further NMR and ESI-MS analysis
349 performed on pre-purified fractions obtained by liquid-liquid partition.

350 Thymol is one of the main components of oregano essential oil (Khan et al., 2019), and rosmarinic acid
351 is reported to be the main phenolic acid found in oregano extracts (Ozkan et al., 2010). In addition to be
352 important for oregano flavor, thymol is also relevant for its numerous biological activities (Dheer et al.,

2019). Rosmarinic acid is another important bioactive metabolite of oregano, especially for its antioxidant potential (Guitard et al., 2016; Villalva et al., 2018).

Besides thymol and rosmarinic acid, p-cymene (VIP 1.02; δ 0.98) and apigenin (VIP 0.85; δ 6.51) were also relevant to predict *O. onites* degree of purity. Conversely, salvianolic acid B (VIP 0.5; δ 6.35) was not strongly correlated to *O. vulgare* degree of purity (Fig. S10 reports the molecular structures of all the compounds mentioned).

3.3 Detection of *Cistus creticus* impurity

Cistus was the most frequent adulterant identified by MA from its characteristic trichomes (Fig. 5A). The adulteration of oregano with cistus, specifically *Cistus creticus* (ex. *incanus*) L., has been also reported by Marieschi et al., 2010. In order to get the adequate model for the prediction of cistus contamination, samples with specific percentage of cistus were prepared in laboratory, spiking *O. onites* and *O. vulgare* samples with diverse cistus percentage (from 2 to 60 %) (Fig. 5A). The NMR-metabolomic profile of these samples was added to the dataset, previously constituted only by the samples provided by the companies. An OPLS model was built using as y variable the percentage of cistus (found in the samples by MA, and known in the samples prepared in laboratory). The model was fitted by four components, with $R^2x(\text{cum}) = 76.9\%$, $R^2y(\text{cum}) = 93.2\%$, $Q^2(\text{cum}) = 88.9\%$, and it was further validated by $R^2(\text{cum})$ and $Q^2(\text{cum})$ obtained by permutation test (200 permutations) (Fig. S13), which were 93.2% and 88.9%, respectively, Q -line intercept on y axis was -0.518 and R -line intercept was 0.198, while $F = 47.2$ and $p = 6.77 \times 10^{-20}$ given by CV-ANOVA. This OPLS model showed a correlation between samples metabolomic profiles and the used y variable. The analysis of the S -plot (Fig. 5B) highlighted a correlation between percentage of cistus contamination and the intensity of a specific ^1H NMR bucket (from δ 3.45 to 3.49; VIP = 5.16). In fact, the spectral signal resonating at δ

376 3.47 was present only in ^1H NMR spectra of contaminated samples. *J-res* experiment confirmed that
377 this signal was a singlet (Fig. S14). Hence, a sample of *Cistus creticus* L. was harvested and analyzed
378 by ^1H NMR profiling, exhibiting a prominent signal at δ 3.47, which confirmed the result given by the
379 OPLS model (Fig. 5C). Through a pre-purification procedure, performed on cistus extract, it was
380 obtained a fraction containing a compound, whose positive ESI-MS yield m/z : 195 $[\text{M} + \text{H}]^+$,
381 calculated as 194.18 for $\text{C}_7\text{H}_{14}\text{O}_6$ and negative ESI-MS was m/z : 193 $[\text{M} - \text{H}]^-$, corresponding to pinitol
382 molecular weight. This cyclic alcohol, in fact, presents a singlet in NMR spectrum at δ 3.47, due to the
383 methoxy group in position 3 of the ring.

384 4. Conclusions

385 Combining results obtained from morphological analysis and ^1H NMR metabolomics, it was possible
386 to rapidly identify non-marketable species of oregano, as well as to discriminate between the two
387 marketable ones (*Origanum vulgare* and *O. onites*). Apigenin and p-cymene were the main biomarkers
388 of *O. onites*, while salvianolic acid B of *O. vulgare*. The developed PCA model was also able to
389 individuate samples made up of a blend of these two species.

390 Moreover, sample degree of purity could be predicted by OPLS. Thymol and rosmarinic acid were very
391 important indicators to predict general oregano purity, together with the specie-specific apigenin, p-
392 cymene. A further model was built to detect the degree of cistus contamination.

393 Metabolomics proved to be a valuable approach for oregano quality control, giving information about
394 oregano species and phytochemical composition of samples, which is an important data, also correlated
395 to the organoleptic properties. The obtained results encourage the use of metabolomics to make
396 predictions regarding oregano quality on the basis of samples NMR profile, supporting also the
397 possibility of building NMR metabolomics-based databases, to be used worldwide for oregano quality
398 control, giving a significant number of information in a considerably short period of time.

399 **Acknowledgment**

400 Thanks are due to Dr. David Baldo from Electron Microscopy Laboratory (DISTAL - Plant Pathology,
401 University of Bologna, V.le Fanin 40, 40127, Bologna, Italy) for the picture with Scanning Electron
402 Microscopy.

403 Thanks are due to Dr. Luca Zuppiroli from Department of Industrial Chemistry (University of Bologna,
404 Viale del Risorgimento, 4, 40136 Bologna, Italy) for technical assistance with ESI-MS experiments.

405 **Conflict of interest**

406 None

407

408 **References**

409 American spice trade. Association, ASTA cleanliness specifications for spices, seeds and herbs,
410 <http://www.ina.or.id/knoma-hpsp/herb/HPSP-12-Ollop> (Accessed September 9, 2020)

411 Anđelković, B., Vujisić, L., Vučković, I., Tešević, V., Vajs, V., & Godevac, D. (2017). Metabolomics
412 study of Populus type propolis. *Journal of Pharmaceutical and Biomedical Analysis*, *135*, 217–226.
413 <https://doi.org/10.1016/j.jpba.2016.12.003>

414 Black, C., Haughey, S. A., Chevallier, O. P., Galvin-King, P., & Elliott, C. T. (2016). A comprehensive
415 strategy to detect the fraudulent adulteration of herbs: The oregano approach. *Food Chemistry*, *210*,
416 551–557. <https://doi.org/10.1016/j.foodchem.2016.05.004>

417 Drabova, L., Alvarez-Rivera, G., Suchanova, M., Schusterova, D., Pulkrabova, J., Tomaniova, M.,
418 Kocourek, V., Chevallier, O., Elliot, C., & Hajslova, J. (2019). Food fraud in oregano: Pesticide

- 419 residues as adulteration markers. *Food Chemistry*, 276, 726–734.
420 <https://doi.org/10.1016/j.foodchem.2018.09.143>
- 421 Dheer, D., Singh, D., Kumar, G., Karnatak, M., Chandra, S., Prakash Verma, V., & Shankar, R. (2019).
422 Thymol Chemistry: A Medicinal Toolbox. *Current Bioactive Compounds*, 15(5), 454–474.
423 <https://doi.org/10.2174/1573407214666180503120222>
- 424 Emwas, A.H., Roy, R., McKay, R.T., Tenori, L., Saccenti, E., Gowda, G.A., Raftery, D., Alahmari, F.,
425 Jaremko, L., Jaremko, M. and Wishart, D.S. (2019). NMR spectroscopy for metabolomics
426 research. *Metabolites*, 9(7), 123. <https://doi.org/10.3390/metabo9070123>
- 427 European Pharmacopoeia (2017). (9th edition) pp.1464–1466
- 428 European Spice Association, Quality Minima Document (2015). [http://www.esa-spices.org/index-](http://www.esa-spices.org/index-esa.html/publications-esa)
429 [esa.html/publications-esa](http://www.esa-spices.org/index-esa.html/publications-esa) (Accessed September 9, 2020)
- 430 European Spice Association, List of culinary herbs and spices (2018). [https://www.esa-](https://www.esa-spices.org/index-esa.html/publications-esa)
431 [spices.org/index-esa.html/publications-esa](https://www.esa-spices.org/index-esa.html/publications-esa) (Accessed September 9, 2020)
- 432 Exarchou, V., Godejohann, M., van Beek, T. A., Gerothanassis, I. P., & Vervoort, J. (2003). LC-
433 UV-solid-phase extraction-NMR-MS combined with a cryogenic flow probe and its application to
434 the identification of compounds present in Greek oregano. *Analytical Chemistry*, 75(22), 6288–
435 6294. <https://doi.org/10.1021/ac0347819>
- 436 Galvin-King, P., Haughey, S. A., & Elliott, C. T. (2018). Herb and spice fraud; the drivers, challenges
437 and detection. *Food Control*, 88, 85–97. <https://doi.org/10.1016/j.foodcont.2017.12.031>
- 438 ISO Online browsing platform. <https://www.iso.org/obp/ui/#iso:std:29207:en> (Accessed September 9,
439 2020)

- 440 Guitard, R., Paul, J. F., Nardello-Rataj, V., & Aubry, J. M. (2016). Myricetin, rosmarinic and carnosic
441 acids as superior natural antioxidant alternatives to α -tocopherol for the preservation of omega-3 oils.
442 *Food Chemistry*, 213, 284–295. <https://doi.org/10.1016/j.foodchem.2016.06.038>
- 443 Ietswaart, J. H. (1980). *A taxonomic revision of the genus Origanum (Labiatae)* (Vol. 4). The Hague:
444 Leiden University Press.
- 445 Khan, M., Khan, S. T., Khan, M., Mousa, A. A., Mahmood, A., & Alkhatlan, H. Z. (2019). Chemical
446 diversity in leaf and stem essential oils of *Origanum vulgare* L. and their effects on microbicidal
447 activities. *AMB Express*, 9(1), 176. <https://doi.org/10.1186/s13568-019-0893-3>
- 448 Malzert-Fréon, A., Hennequin, D., & Rault, S. (2010). Partial least squares analysis and mixture design
449 for the study of the influence of composition variables on lipidic nanoparticle characteristics. *Journal*
450 *of Pharmaceutical Sciences*, 99(11), 4603–4615. <https://doi.org/10.1002/jps.22177>
- 451 Mandrone, M., Scognamiglio, M., Fiorentino, A., Sanna, C., Cornioli, L., Antognoni, F., Bonvicini, F.
452 & Poli, F. (2017). Phytochemical profile and α -glucosidase inhibitory activity of Sardinian *Hypericum*
453 *scruglii* and *Hypericum hircinum*. *Fitoterapia*, 120, 184–193.
454 <https://doi.org/10.1016/j.fitote.2017.06.020>
- 455 Mandrone, M., Antognoni, F., Aloisi, I., Potente, G., Poli, F., Cai, G., Faleri, C., Parrotta, L., & Del
456 Duca, S. (2019). Compatible and incompatible pollen-styles interaction in *Pyrus communis* L. show
457 different transglutaminase features, polyamine pattern and metabolomics profiles. *Frontiers in Plant*
458 *Science*, 10, 741. <https://doi.org/10.3389/fpls.2019.00741>
- 459 Mandrone, M., Chiocchio, I., Barbanti, L., Tomasi, P., Tacchini, M. and Poli, F., 2021. Metabolomic
460 study of sorghum (*Sorghum bicolor*) to interpret plant behavior under variable field conditions in view

- 461 of smart agriculture applications. *Journal of Agricultural and Food Chemistry*, 69(3), 1132-1145.
462 <https://doi.org/10.1021/acs.jafc.0c06533>
- 463 Marieschi, M., Torelli, A., Poli, F., Sacchetti, G., & Bruni, R. (2009). RAPD-based method for the
464 quality control of Mediterranean oregano and its contribution to pharmacognostic techniques. *Journal*
465 *of Agricultural and Food Chemistry*, 57(5), 1835–1840. <https://doi.org/10.1021/jf8032649>
- 466 Marieschi, M., Torelli, A., Poli, F., Bianchi, A., & Bruni, R. (2010). Quality control of commercial
467 Mediterranean oregano: Development of SCAR markers for the detection of the adulterants *Cistus*
468 *incanus* L., *Rubus caesius* L. and *Rhus coriaria* L. *Food Control*, 21(7), 998–1003.
469 <https://doi.org/10.1016/j.foodcont.2009.12.018>
- 470 Marieschi, M., Torelli, A., Bianchi, A., & Bruni, R. (2011). Development of a SCAR marker for the
471 identification of *Olea europaea* L.: A newly detected adulterant in commercial Mediterranean oregano.
472 *Food Chemistry*, 126(2), 705–709. <https://doi.org/10.1016/j.foodchem.2010.11.030>
- 473 Marieschi, M., Torelli, A., Bianchi, A., & Bruni, R. (2011). Detecting *Satureja montana* L. and
474 *Origanum majorana* L. by means of SCAR–PCR in commercial samples of Mediterranean oregano.
475 *Food Control*, 22(3-4), 542–548. <https://doi.org/10.1016/j.foodcont.2010.10.001>
- 476 Ozkan, G., Baydar, H. and Erbas, S. (2010). The influence of harvest time on essential oil composition,
477 phenolic constituents and antioxidant properties of Turkish oregano (*Origanum onites* L.). *Journal of*
478 *the Science of Food and Agriculture*, 90(2), 205–209. <https://doi.org/10.1002/jsfa.3788>
- 479 Pontes, J. G. M., Brasil, A. J. M., Cruz, G. C., de Souza, R. N., & Tasic, L. (2017). NMR-based
480 metabolomics strategies: plants, animals and humans. *Analytical Methods*, 9(7), 1078–1096.
481 <https://doi.org/10.1039/C6AY03102A>

- 482 Riedl, J., Esslinger, S., & Fahl-Hassek, C. (2015). Review of validation and reporting of non-targeted
483 fingerprinting approaches for food authentication. *Analytica Chimica Acta*, 885, 17–32.
484 <https://doi.org/10.1016/j.aca.2015.06.003>
- 485 Sun, Y., Zhu, H., Wang, J., Liu, Z. and Bi, J., 2009. Isolation and purification of salvianolic acid A and
486 salvianolic acid B from *Salvia miltiorrhiza* by high-speed counter-current chromatography and
487 comparison of their antioxidant activity. *Journal of Chromatography B*, 877(8-9), pp.733–737.
488 <https://doi.org/10.1016/j.jchromb.2009.02.013>
- 489 Salomé-Abarca, L. F., Mandrone, M., Sanna, C., Poli, F., van der Hondel, C. A., Klinkhamer, P. G., &
490 Choi, Y. H. (2020). Metabolic variation in *Cistus monspeliensis* L. ecotypes correlated to their plant-
491 fungal interactions. *Phytochemistry*, 176, 112402. <https://doi.org/10.1016/j.phytochem.2020.112402>
- 492 Scognamiglio, M., D'Abrosca, B., Esposito, A., & Fiorentino, A. (2015). Chemical composition and
493 seasonality of aromatic mediterranean plant species by NMR-based metabolomics. *Journal of*
494 *Analytical Methods in Chemistry*, 2015. <https://doi.org/10.1155/2015/258570>
- 495 Sobolev, A. P., Thomas, F., Donarski, J., Ingallina, C., Circi, S., Marincola, F. C., Capitani, D., &
496 Mannina, L. (2019). Use of NMR applications to tackle future food fraud issues. *Trends in Food*
497 *Science & Technology*, 91, 347–353. <https://doi.org/10.1016/j.tifs.2019.07.035>
- 498 Van Ruth, S. M., Luning, P. A., Silvis, I. C., Yang, Y., & Huisman, W. (2018). Differences in fraud
499 vulnerability in various food supply chains and their tiers. *Food Control*, 84, 375–381.
500 <https://doi.org/10.1016/j.foodcont.2017.08.020>
- 501 Villalva, M., Jaime, L., Aguado, E., Nieto, J. A., Reglero, G., & Santoyo, S. (2018). Anti-inflammatory
502 and antioxidant activities from the basolateral fraction of Caco-2 cells exposed to a rosmarinic acid

503 enriched extract. *Journal of Agricultural and Food Chemistry*, 66(5), 1167–1174.
504 <https://doi.org/10.1021/acs.jafc.7b06008>

505 Wadood, S. A., Boli, G., Xiaowen, Z., Hussain, I., & Yimin, W. (2020). Recent development in the
506 application of analytical techniques for the traceability and authenticity of food of plant origin.
507 *Microchemical Journal*, 152, 104295. <https://doi.org/10.1016/j.microc.2019.104295>

508

Journal Pre-proof

Fig. 1 A) Morphological differences between *O. vulgare* e *O. onites* calix, and NMR-based PCA score scatter plot, *O. onites* (blue dots) is distinguished by *O. vulgare* (red dots) along the component t[1], samples composed by a mixture of both species (violet dots) are placed in the middle. B) OPLS-DA score scatter plot using *O. onites* and *O. vulgare* as model classes (blended samples and samples with percentage of contamination higher than 15% were excluded from this model). C) PCA score scatter plot including two samples (green dots) resulted non-marketable by MA, which are outliers. Each sample was analyzed in duplicate (blended samples were excluded from the dataset).

Fig. 2 ¹H NMR spectra of *O. vulgare* (on top) and *O. onites* (bottom). Extended spectral regions are shown on top of the figure. Numbers indicate the diagnostic signals of the main metabolites: 1 = p-cymene, 2 = thymol, 3 = alanine, 4 = quinic acid, 5 = acetic acid, 6 = malic acid, 7 = aspartic acid, 8 = sucrose, 9 = β -glucose, 10 = rosmarinic acid, 11 = α -glucose, 12 = salvianolic acid B, 13 = apigenin, 14 = formic acid, 15 = unknown compound.

Fig. 3 A) PCA score scatter plot where unknown samples (yellow dots) are discriminated from the two marketable oregano species. **B) Structures of thymol and carvacrol**, resulting the main compounds determining the discrimination of these samples **C) Aliphatic region of ¹H NMR spectra of marketable oregano**, thymol characteristic spectral signals are present only in the marketable species, while the unknown species presents carvacrol instead of thymol.

Fig. 4 OPLS score scatter plot (on top) and observed vs predicted plot (bottom). Percentage of total impurity of **A) *O. vulgare*** and **B) *O. onites*** was used as y variable. Samples were analyzed in duplicate. Samples constituted by unknown species or a mixture of the two marketable species were excluded from this analysis.

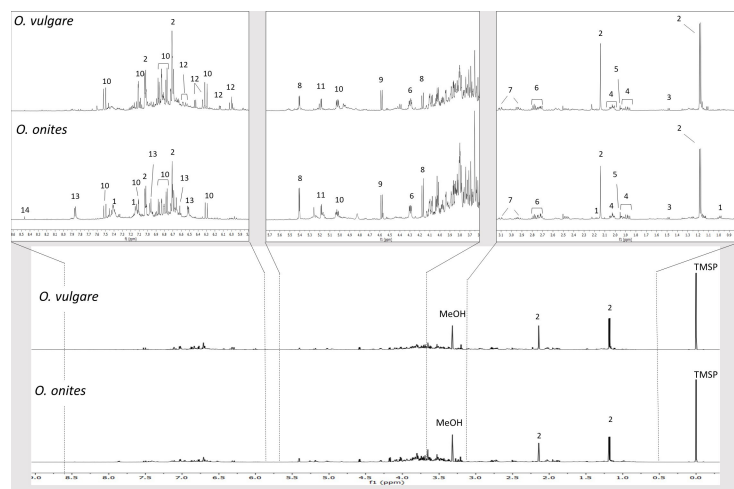
Fig. 5 A) Different trichomes of cistus (on the right) and oregano (on the left) and OPLS score scatter plot (y variable was percentage of cistus). The shift along component t[1] is due to oregano species: *O. onites* samples (dots) are placed on positive t[1], and *O. vulgare* (squares) are placed on negative t[1] of the model. Percentage of cistus contamination is given along the component t[0]. **B) OPLS S-Plot**, which indicates the ¹H NMR bin at δ 3.45-3.49 as strongly correlated to cistus contamination. **C) Extended ¹H**

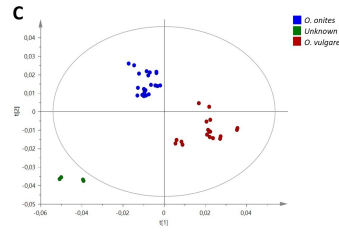
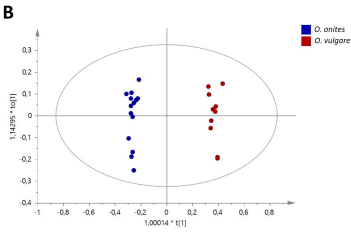
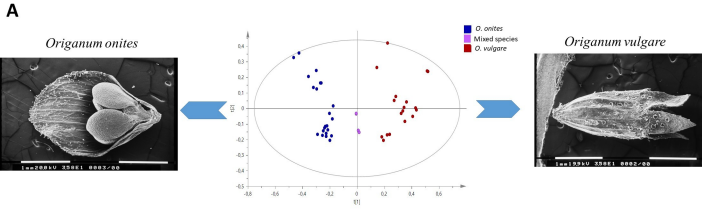
NMR spectral region of *Cistus creticus* showing an evident signal at δ 3.47, due to the methoxy group of pinitol.

Table 1. Vouchers, origin, and results of the morphological analysis (MA) performed on the samples analyzed in this work. Samples were provided by different companies, who received, in turn, from third parties, who give the information related to sample origin. Samples defined as ‘unknown’ species have to be considered non-marketable as oregano. Samples coming from Sicily were identified as *O. vulgare* by MA while as ‘unknown’ species by NMR-metabolomics (this information has been reported in the Table).

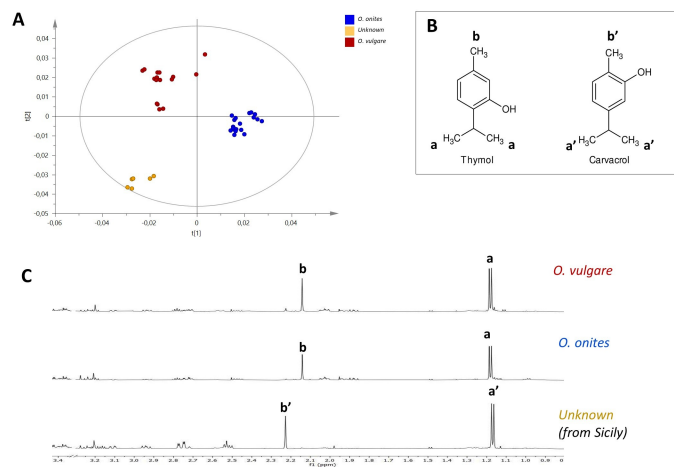
Vo uch ers	Origin	total orega no (%)	leaf and flowe r (%)	stem (%)	total impuri ty (%)	other Labiatae (%)	other plants (%)	cistus (%)	non- plant materi al (%)	oli ve lea ves (%)	Species
BO 1A0 01	Turkey	85.28	81.06	4.22	14.72	13.62	1.1	0	0	0	<i>O. onites + O.vulga re</i>
BO 2B OR	Sicily	97.68	94.40	3.28	2.32	0	2.32	0	0	0	<i>O. vulgare (by MA); unknow n (by metabol omics)</i>
BO 3C OR	Turkey	96.6	87.56	9.04	3.4	2.6	0.8	0	0	0	<i>O. onites</i>
BO 4D OR	Turkey	90.16	83.20	6.96	9.84	9.1	0.44	0	0.3	0	<i>O. onites</i>
BO 5E OR	Peru	99.72	97.40	2.32	0.28	-	0	0	0.28	0	unknow n
BO 6F OR	Turkey	99.88	96.60	3.28	0.12	0	0	0	0.12	0	<i>O. onites</i>
BO 7G OR	Turkey	98.4	94.12	4.28	1.6	0	1.6	0	0	0	<i>O. onites</i>
BO 8H OR	Turkey	98.26	91.58	6.68	1.74	1.7	0.04	0	0	0	<i>O. onites</i>
BO 9IO R	Not declared	49.14	43.44	5.70	50.86	0.52	0	50.34	0	0	<i>O. onites</i>
BO 10L OR	Turkey	95.82	91.82	4.00	4.18	4.02	0	0.16	0	0	<i>O. onites</i>
BO 11 MO R	Turkey	98.58	90.40	8.18	1.42	0.7	0.2	0.52	0	0	<i>O. onites</i>
BO 12N OR	Turkey	81.7	75.14	6.56	18.3	5.9	10.54	1.86	0	10. 54	<i>O. onites</i>
BO 13O OR	Turkey	74.46	69.88	4.58	25.54	7.6	7.42	10.52	0	7.4 2	<i>O. onites</i>
BO 14P OR	Turkey	77.18	74.14	3.04	22.82	3.98	7.6	11.24	0	7.6	<i>O. onites</i>
BO 15Q OR	Turkey	93.82	88.12	5.70	6.18	4.7	1.48	0	0	0	<i>O. vulgare</i>
BO 16R OR	Turkey	67.64	62.94	4.70	32.36	0	1.4	30.96	0	0	<i>O. vulgare</i>

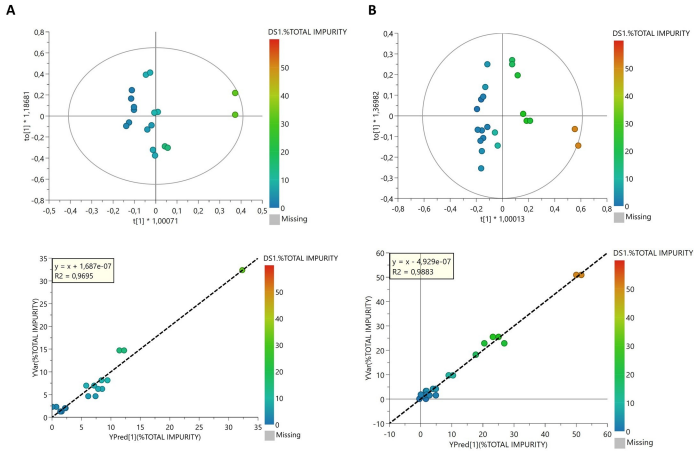
BO 17S OR	Albania	85.26	75.76	8.83	14.74	6.04	8.53	0.16	0	0	<i>O. vulgare</i>
BO 18T OR	Not declared	95.36	86.52	8.60	4.64	2.4	2.1	0	0	0	<i>O. vulgare</i>
BO 19U OR	Albania	98	86.70	11.30	2	1	1	0	0	0	<i>O. vulgare</i>
BO 20V OR	Peru	99.94	97.24	2.70	0.06	-	0	0	0.06	0	unknown
BO 21Z OR	Albania	98.74	90.12	8.62	1.26	0.74	0.52	0	0	0	<i>O. vulgare</i>
BO 22A AO R	Turkey	98.96	88.96	10.00	1.04	0.18	0.86	0	0	0	<i>O. onites + O. vulgare</i>
BO 23A BO R	Not declared	96.66	89.86	6.80	2.34	0	2.34	0	0	0	<i>O. vulgare</i>
BO 24A CO R	Sicily	100	97.42	2.58	0	0	0	0	0	0	<i>O. vulgare</i> (by MA); unknown (by metabolomics)
BO 25A DO R	Not declared	91.8	86.08	5.72	8.2	7.12	0	0	0	0	<i>O. vulgare</i>
BO 26A EO R	Not declared	93.02	80.88	12.14	6.98	6.18	0	0	0	0	<i>O. vulgare</i>
BO 27A FO R	Sicily	97.48	95.10	2.38	2.52	0	2.2	0	0.3	0	<i>O. vulgare</i> (by MA); unknown (by metabolomics)



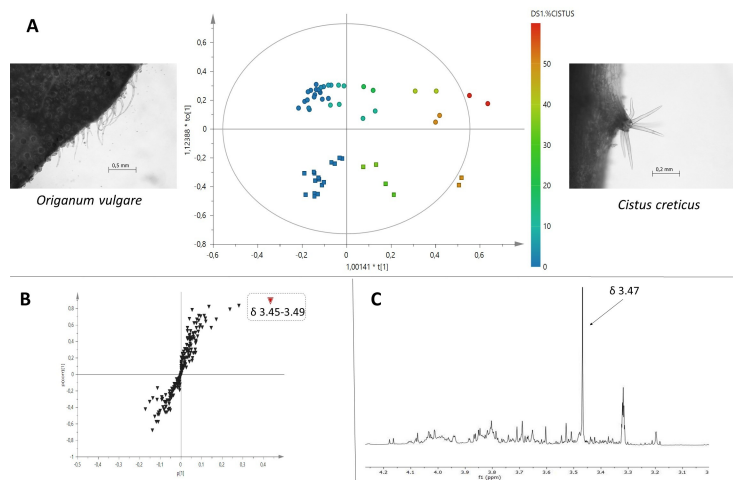


Journal Pre-proof





Journal Pre-proof



Highlights

- Oregano is one of the most counterfeited spices
- Nuclear Magnetic Resonance-based metabolomics detect frauds in oregano samples
- Metabolomics provided species-specific biomarkers of *Origanum onites* and *O. vulgare*
- Metabolomics allowed to predict oregano degree of purity

Journal Pre-proof

Declaration of interests

The authors declare that they have no known competing financial interests or personal relationships that could have appeared to influence the work reported in this paper.

The authors declare the following financial interests/personal relationships which may be considered as potential competing interests:

Journal Pre-proof